An autonomous, but INSIG-modulated, role for the sterol sensing domain in mallostery-regulated ERAD of yeast HMG-CoA reductase

Margaret A. Wangeline⬤ and Randolph Y. Hampton*⬤

From the Division of Biological Sciences, the Section of Cell and Developmental Biology, UCSD, La Jolla, California, USA

Edited by Phyllis Hanson

HMG-CoA reductase (HMGR) undergoes feedback-regulated degradation as part of sterol pathway control. Degradation of the yeast HMGR isozyme Hmg2 is controlled by the sterol pathway intermediate GGPP, which causes misfolding of Hmg2, leading to degradation by the HRD pathway; we call this process mallostery. We evaluated the role of the Hmg2 sterol sensing domain (SSD) in mallostery, as well as the involvement of the highly conserved INSIG proteins. We show that the Hmg2 SSD is critical for regulated degradation of Hmg2 and required for mallosteric misfolding of GGPP as studied by *in vitro* limited proteolysis. The Hmg2 SSD functions independently of conserved yeast INSIG proteins, but its function was modulated by INSIG, thus imposing a second layer of control on Hmg2 regulation. Mutant analyses indicated that SSD-mediated mallostery occurred prior to and independent of HRD-dependent ubiquitination. GGPP-dependent misfolding was still extant but occurred at a much slower rate in the absence of a functional SSD, indicating that the SSD facilitates a physiologically useful rate of GGPP response and implying that the SSD is not a binding site for GGPP. Nonfunctional SSD mutants allowed us to test the importance of Hmg2 quaternary structure in mallostery: a nonresponsive Hmg2 SSD mutant strongly suppressed regulation of a coexpressed, normal Hmg2. Finally, we have found that GGPP-regulated misfolding occurred in detergent-solubilized Hmg2, a feature that will allow next-level analysis of the mechanism of this novel tactic of ligand-regulated misfolding.

Endoplasmic reticulum(ER)-associated degradation (ERAD) refers to a conserved set of degradation pathways that detect and degrade misfolded, unassembled, and damaged ER-resident proteins (1–4). Both luminal (ERAD-L) and integral membrane (ERAD-M) proteins can be subject to ERAD. ERAD is initiated by the action of a surprisingly small set of conserved E3 ubiquitin ligases that each recognize a large range of substrates. The two major ERAD pathways in yeast—defined by the participant ligases—are the HRD (pronounced "herd") pathway and the DOA (pronounced "dee-oh-ay") pathway. The detailed structural features of an ERAD substrate that determine HRD- or DOA-dependent degradation are being unraveled and appear to encompass a large number of variations from wild-type stable configuration. Despite the large variety of possible substrates accommodated by each pathway, ERAD displays high specificity for misfolded versions of the proteins that undergo degradation, as would be required for an evolutionarily successful quality control pathway.

In the course of our studies on the sterol synthetic pathway in yeast, we discovered that the HRD ERAD quality control pathway is also used to regulate levels of the normal, rate-limiting sterol synthetic enzyme HMG-CoA reductase (HMGR) (5–7). Specifically, the Hmg2 isozyme undergoes negative feedback regulation effected at the level of HRD-dependent degradation: the 20-carbon sterol pathway molecule geranylgeranyl pyrophosphate (GGPP) accelerates HRD-dependent degradation of Hmg2, thus allowing control over Hmg2 levels keyed to changing cellular demand for sterol pathway products. Interestingly, although the regulatory mechanisms are distinct, mammalian HMGR stability is also controlled in part by GGPP-mediated enhancement of degradation by ER-localized E3 ligases (8).

Like other quality control pathways, HRD-mediated ERAD is highly specific for misfolded versions of its many protein substrates. Our studies have revealed that the high selectivity of the HRD pathway for misfolded versions of substrates underlies HRD-dependent regulation of Hmg2 stability by GGPP: when GGPP levels are elevated, Hmg2 undergoes a reversible structural transition to a more misfolded form, allowing enhanced recognition and destruction by the HRD pathway and consequent lowering of Hmg2 activity. It appears that this mode of regulation by quality control has many examples throughout biology (9–16). Furthermore, the presence of numerous degradative quality control pathways in all cellular compartments allows for the possibility of translational applications of regulated quality control in which small molecules that program quality control degradation of desired targets could be discovered and developed. Accordingly, we have devoted significant energy toward understanding the mechanisms at play in the GGPP-mediated enhancement of HRD-dependent Hmg2 degradation.

We have employed a variety of approaches to observe that GGPP causes reversible misfolding of the Hmg2 protein to enhance HRD-dependent Hmg2 degradation (17–19). Using

---

This article contains supporting information.
* For correspondence: Randolph Y. Hampton, rhampton@ucsd.edu.

both *in vivo* and *in vitro* methods, we found that the effects of GGPP on Hmg2 structure are remarkably similar to allosteric regulation. Because of these similarities, we have named this ligand-based misfolding "mallostery," a portmanteau combining the ideas of misfolding with those of allosteric regulation to refer to this type of highly specific ligand-mediated misfolding (13, 18).

In our studies of mallostery, we built the case for the allosteric analogy in Hmg2-regulated degradation, showing high potency and structural specificity of GGPP, providing evidence of specific binding indicated by a close analog—GGSPP—that functions as a GGPP antagonist, and demonstrating that reversible misfolding is central to GGPP's role as an indicator of sterol pathway activity. In the studies below, we examined the in-cis features of Hmg2 regulation by GGPP, using a variety of Hmg2 mutants with highly specific lesions in degradative behavior to both explore the nature of ligand-mediated misfolding and further test the mallosteric model. We paid particular attention to the highly conserved sterol sensing domain (SSD), found in many proteins that pertain to sterol response, synthesis, or transport. The data indicated that the SSD functions as an autonomous motif to promote mallosteric misfolding. Furthermore, the mutants described in these studies allowed a strong test of the importance of the multimeric structure in ligand-regulated Hmg2 misfolding. Finally, we demonstrate that mallosteric regulation of Hmg2 can occur in detergent-solubilized Hmg2, setting the stage for next-level experiments to both understand and harness this highly specific regulatory strategy in both fundamental and translational endeavors.

Results

The sterol sensing domain (SSD) is required for ligand-regulated Hmg2 misfolding

The SSD is a motif found in the multispanning membrane domains of many proteins that function in sterol synthesis, response, or regulation, including yeast Hmg2 (13, 19–22). This highly conserved motif occurs in the intra- and juxta-membrane residues over five adjacent membrane-spanning alpha helices. Often, mutation of highly conserved SSD residues alters the regulatory or functional responses of SSD-containing proteins (19, 23, 24). Our previous work identified several conserved residues in the SSD of Hmg2 that are required for Hmg2-regulated degradation (Fig. 1A) (19). Surprisingly, all SSD mutations that caused changes in Hmg2 degradation, including mutation of the highly conserved S215 residue to A, produced *increased* stability over wild-type (19), in contrast to the usual role of strongly conserved residues in permitting maximal stability. We had earlier noted that the S215A mutation also blocked the response to the putative regulatory ligand farnesol (FOH) in an *in vitro* limited proteolysis assay of Hmg2 structure. Later work demonstrated that the *bona fide* signal for Hmg2-regulated degradation is the highly potent, mallosteric regulator geranylgeranyl pyrophosphate (GGPP), which is effective at concentrations approximately 1000 times lower than FOH (18, 25). Accordingly, we

examined the importance of these phenotypic, conserved SSD mutations on physiologically relevant, GGPP-induced reversible misfolding of Hmg2, using both *in vivo* and *in vitro* approaches.

To study the role of the Hmg2 SSD *in vivo* and *in vitro*, we employed the Hmg2-GFP reporter, in which the C-terminal catalytic domain of Hmg2 is replaced by GFP (Fig. 1B). Hmg2-GFP lacks HMG-CoA reductase catalytic activity but undergoes quantitatively normal regulated degradation (18, 25, 26). We focused on the mutants with the strongest phenotype from our earlier broad survey of this motif. The two mutants featured herein, S215A and L219F, each showed a loss of response to direct addition of the degradation signal GGPP to living cells. Both mutants were nonresponsive to GGPP addition compared with wild-type Hmg2-GFP (Fig. 1C). Similarly, both mutants displayed the expected strong stabilization after addition of cycloheximide, whereas the wild-type protein displayed a drop in steady-state levels due to degradation stimulated by the natural ambient concentration of GGPP (Fig. 1D) (19). This lack of degradation in response to GGPP can be further assayed by direct addition of GGPP to cells during cycloheximide chase to stimulate HRD-dependent Hmg2 degradation (18, 25). Again, the two mutants were essentially nonresponsive to GGPP addition (Fig. 1D). This confirmed that the GGPP-stimulated degradation showed the expected dependence on highly conserved SSD residues predicted from our earlier studies, allowing us to delve more deeply into the role of this motif in mallosteric control of Hmg2 folding.

To that end, we employed a limited proteolysis assay of Hmg2, involving a myc-tagged version of Hmg2-GFP called 1myc$_L$-Hmg2-GFP—developed early in our studies of regulated degradation—in our analysis of the SSD. The myc tag in 1myc$_L$-Hmg2-GFP is present in the first luminal loop of Hmg2 and so is protected by the ER membrane, allowing detection of the protein and its cleavage products after proteolytic treatment of Hmg2 in isolated microsomes (Fig. 2A). Importantly, 1myc$_L$-Hmg2-GFP is regulated normally (18, 27, 28). When microsomes prepared from strains expressing 1myc$_L$-Hmg2-GFP are treated with limiting concentrations of trypsin, a characteristic pattern of cleavage fragments is produced that can be detected by blotting for the protected myc tag, an example being shown in Figure 2. When GGPP is included in the proteolysis assay, Hmg2 proteolysis occurs more rapidly (18, 28) (Fig. 2A). Only the rate at which the fragments are produced changes, not the pattern itself (27, 28). The highly stable S215A version of 1myc$_L$-Hmg2-GFP did not respond to added GGPP at any concentration tested, even 2000-fold higher than that required to stimulate misfolding in the wild-type protein (Fig. 2B). Similarly, the stabilizing L219F mutation of that conserved SSD residue also blocked the response to GGPP *in vitro* (Fig. 2C). Thus, it appears that GGPP-dependent misfolding occurred by an SSD-dependent process.

INSIG independence of SSD-dependent mallostery

The SSD is perhaps best known for mediating sterol-dependent binding to the regulatory proteins known as
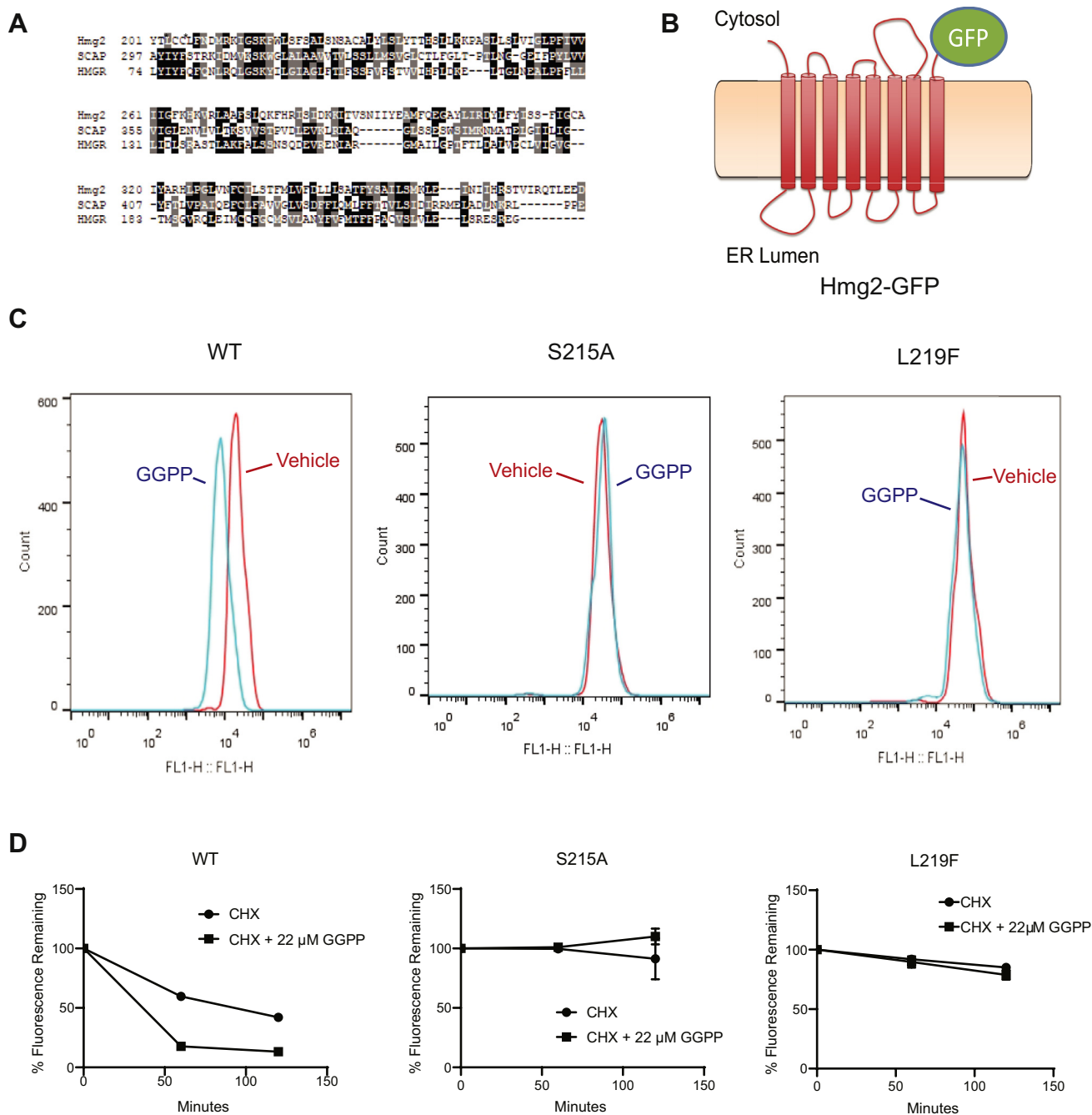
Figure 1. The Hmg2 sterol sensing domain (SSD) was required for GGPP-regulated degradation. *A*, amino acid sequence alignment of *S. cerevisiae* Hmg2 and *H. sapiens* SCAP and HMGR containing the region of the SSD. Similarities are highlighted in *gray*, and identities are highlighted in *black*. Asterisks show the conserved residues S215 and L219. *B*, schematic of the optical reporter Hmg2-GFP. The transmembrane region of Hmg2 is fused to GFP. (Cartoon originally appeared in (18) and used with permission.). *C*, SSD mutations rendered Hmg2 more stable *in vivo*. Histograms of Hmg2-GFP, wild-type, or with the mutations S215A and L219F, as indicated, at steady state (*red*) or after 2 h of cycloheximide treatment (*blue*). *D*, stabilized SSD mutations are GGPP insensitive. Cycloheximide chase of wild-type and the S215A or L219F SSD mutants of Hmg2-GFP, in which CHX is added at time 0, and subsequent levels were measured by flow cytometry, in the presence of vehicle (*solid circles*) or 22 μM GGPP (*solid squares*). Error bars are SEM.

INSIGs (insulin-stimulated genes). In many cases, an SSD–INSIG interaction underlies regulation that requires an SSD (13, 29–33). For example, mammalian HMGR requires SSD-mediated INSIG binding for sterol-regulated degradation (29, 30). Similarly, mammalian SCAP employs SSD-dependent INSIG binding to control the sterol-regulated trafficking that mediates sterol-based control of transcription (33). *S. cerevisiae* has two INSIG homologs called Nsg1 and Nsg2.

Nsg1 binds to Hmg2 in a sterol-dependent manner that strongly inhibits its regulated degradation (31, 32). Accordingly, we wondered if the SSD-dependent, GGPP-stimulated degradation of Hmg2 was in any way dependent on either of the yeast INSIG homologs. Typically, we study Hmg2-regulated degradation at levels of Hmg2 in excess of native promoter-dependent Nsg expression (31). Nevertheless, it was formally possible that the Nsgs were involved in
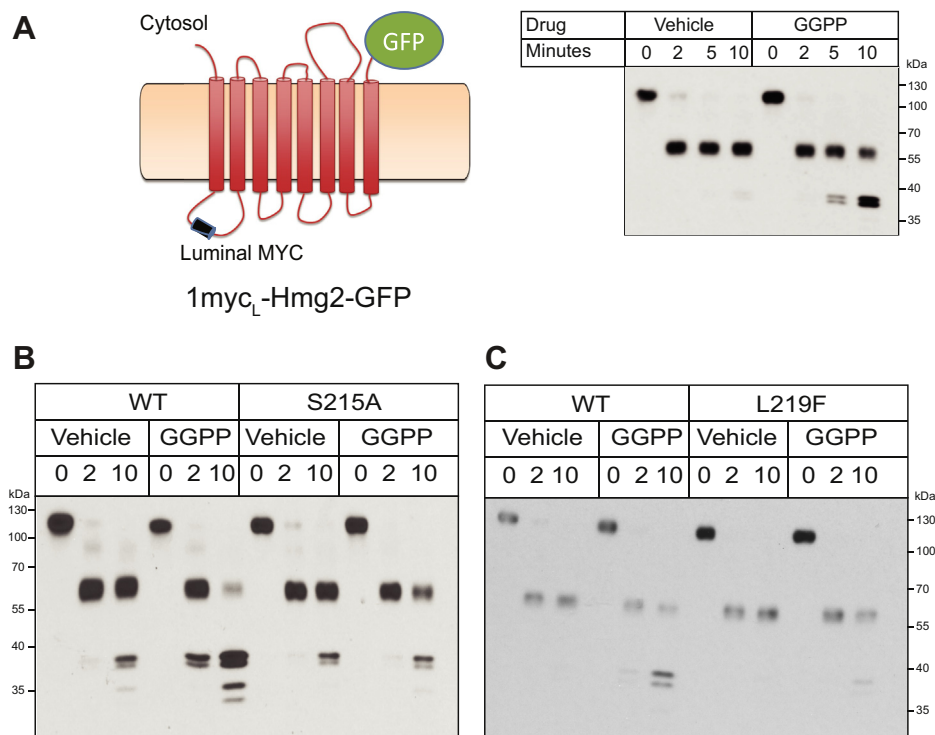
Figure 2. The SSD is required for GGPP-mediated mallosteric misfolding *in vitro*. *A*, left, schematic of the luminally tagged 1myc$_L$-Hmg2-GFP reporter. A myc tag is inserted into the first luminal loop of Hmg2, and the Hmg2 transmembrane region is fused to GFP. (Cartoon first appeared in (18); used by permission) ER/Golgi microsomes were isolated from strains expressing 1myc$_L$-Hmg2-GFP, treated with vehicle or 22 μM GGPP, and subjected to proteolysis with trypsin. Addition of GGPP accelerates the rate of proteolysis approximately fivefold. *B* and *C*, stabilizing SSD mutations blocked GGPP-induced misfolding. Microsomes isolated from strains expressing wild-type or S215A 1myc$_L$-Hmg2-GFP (*B*), or L219F 1myc$_L$-Hmg2-GFP (*C*), were treated with vehicle or GGPP prior to proteolysis and then treated with trypsin for the indicated times followed by immunoblotting for the luminal myc tag. GGPP induced misfolding and increased proteolysis in the wild-type protein, but was essentially ineffective.

SSD-dependent degradation of Hmg2, so we directly tested that possibility.

Simultaneous deletion of Nsg1 and Nsg2 did not affect the steady-state level of Hmg2-GFP as measured by flow cytometry (Fig. 3*A*, left). Furthermore, Hmg2-GFP remained normally responsive to GGPP in *nsg1Δnsg2Δ* double null strains (Fig. 3*A*, right). As a control, we also tested whether INSIG deletion affected the strong acquired stability of the SSD mutant S215A. As expected, S215A Hmg2-GFP levels were unaffected by deletion of both INSIGS, and it remained stable and unresponsive to GGPP in the *nsg1Δnsg2Δ* strain (Fig. 3*B*, left and right, respectively). As expected from our earlier studies, expression of Nsg1 from the same strong promoter as that used for Hmg2-GFP, allowing stoichiometric interaction between the Nsg1 and Hmg2, increased the steady-state level of Hmg2-GFP (Fig. 3*C*, left) and blocked the degradation-stimulating effects of GGPP (Fig. 3*C*, right). We next confirmed that INSIGs were not required for the SSD-dependent response to GGPP using the *in vitro* proteolysis assay. When 1myc$_L$-Hmg2-GFP was expressed in the *nsg1Δnsg2Δ* double null strain, it responded normally to GGPP (Fig. 3*D*, left). Conversely, the presence of high levels of Nsg1 completely blocked GGPP-dependent misfolding of 1myc-Hmg2-GFP (Fig. 3*D*, right). Taken together, these data suggest that yeast INSIGs were not required for SSD-dependent regulated Hmg2 misfolding, but instead blocked the function

of the SSD by binding, which, as we have shown, occurs in a sterol-dependent manner (34). We have previously posited that this combination of regulatory effects allows for "contingency regulation" of Hmg2 ERAD, in which high GGPP and low sterols are the metabolic conditions required for Hmg2 degradation—appropriate for the natural physiology of HMGR in yeast (32). Whatever the evolutionary function of Nsg-mediated blockade of Hmg2 degradation, it is clear that GGPP-dependent mallostery of Hmg2 represents an autonomous, but INSIGs-modulated, physiological function of the Hmg2 SSD.

Separate determinants of Hmg2 mallosteric misfolding and ER degradation

We have previously identified a number of stabilizing mutations in Hmg2 (19, 35). Because regulated degradation of Hmg2 entails ligand-mediated misfolding followed by Hrd1-dependent ubiquitination and degradation, we wondered if any of the various mutations might lesion different parts of this multistep regulatory process. Using the limited proteolysis assay to look specifically at the ligand-regulated misfolding step of Hmg2 regulation, we tested other stabilizing Hmg2 mutations to learn whether they, like conserved SSD residues, alter mallosteric misfolding, or other aspects of Hmg2 ERAD.

We focused on two lysines involved in Hmg2 degradation, K6 and K357, discovered in our early work (36). Each is
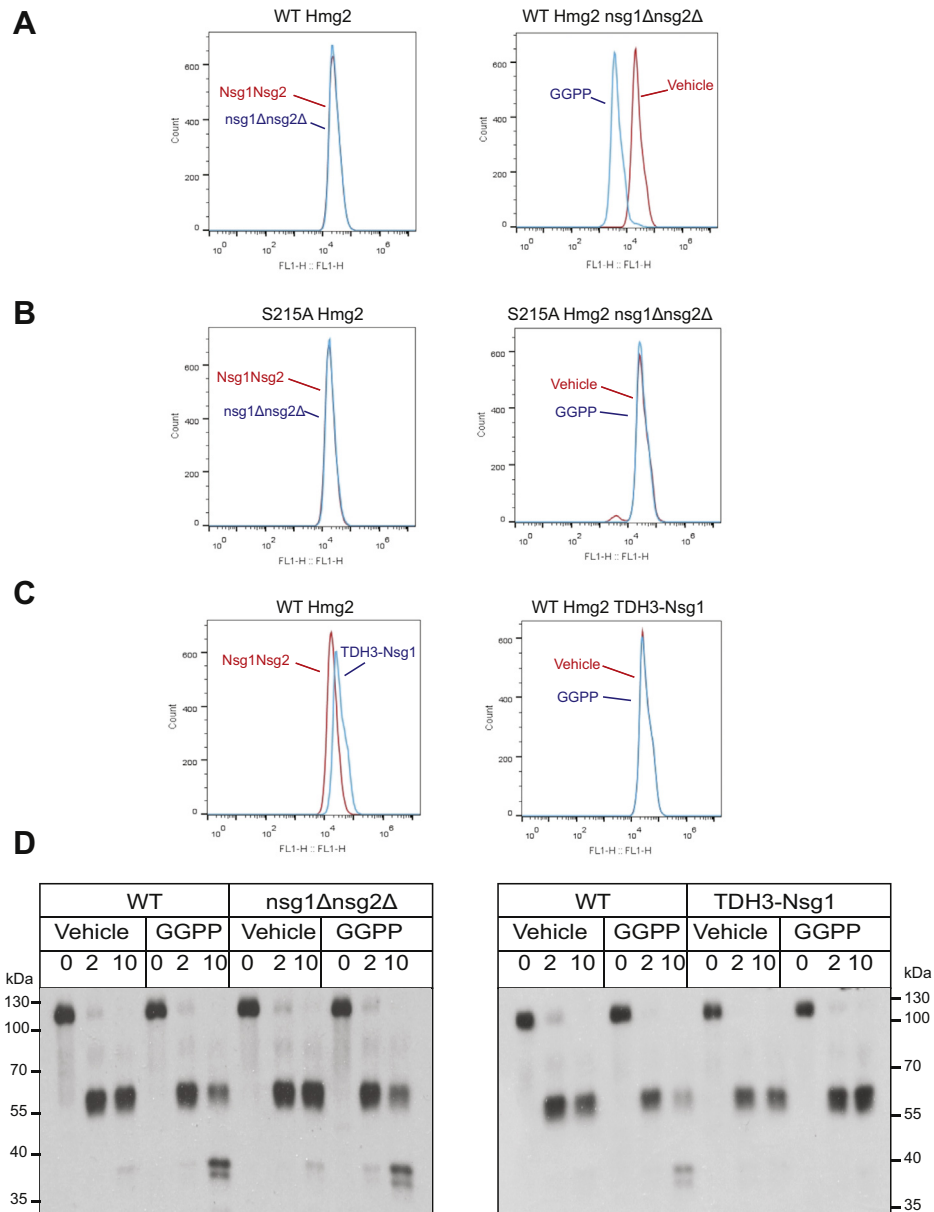
Figure 3. GGPP-regulated Hmg2 mallosteric misfolding did not require INSIG proteins and was inhibited by excess Nsg1. *A* absence of yeast INSIGS Nsg1 and Nsg2 did not affect regulated degradation of Hmg2-GFP. Left panel, steady-state levels of Hmg2-GFP in a strain with wild-type INSIG proteins (red curve) or an otherwise identical strain with missing both INSIG genes by virtue of nsg1Δnsg2Δ double null (*blue curve*). Right panel: in the INSIG double null, 22 μM GGPP treatment caused the expected drop in steady-state Hmg2-GFP levels (*blue curve*) compared with vehicle (*red curve*). *B*, deletion of yeast INSIGs did not alter the stability or GGPP nonresponsiveness of the S215A mutant. Left panel, S215A Hmg2-GFP levels in a wild-type (*red curve*) or nsg1Δnsg2Δ double null strain (*blue curve*). Right panel, lack of GGPP responsiveness of S215A mutant in an nsg1Δnsg2Δ strain treated with vehicle (*red*) or 22 μM GGPP (*blue*) for 1 h. The block in regulation of the S215A mutant was not affected by INSIG deletion. *C*, overexpression of Nsg1 increased Hmg2-GFP levels and prevented GGPP-induced degradation. Left, wild-type Hmg2-GFP expressed in a wild-type strain (*red*) or a strain producing Nsg1 from the strong TDH3 promoter (*blue*) was evaluated for steady-state fluorescence by flow cytometry. Right, cells expressing Hmg2-GFP in an identical strain expressing Nsg1 from the strong TDH3 promoter were treated with vehicle (*red*) or 22 μM GGPP (*blue*) and evaluated for steady-state fluorescence by flow cytometry for 1 h. *D*, GGPP-induced *in vitro* misfolding of Hmg2-GFP did not require INSIGs, but was blocked by strong Nsg1 coexpression. Left, *in vitro* proteolysis of 1myc_L-Hmg2-GFP expressed in wild-type and nsg1Δnsg2Δ yeast. 22 μM GGPP induced misfolding and increased the rate of proteolysis in both backgrounds. Right, *in vitro* proteolysis of 1myc_L-Hmg2-GFP expressed in a strain wild-type for INSIGs and a strain expressing Nsg1 from the strong TDH3 promoter. Co-overexpression of Nsg1 blocked GGPP-induced misfolding.

required for Hmg2-regulated degradation: mutation of either lysine to arginine results in complete stabilization at any concentration of the degradation signal (Fig. 4A) (17, 36, 37). Neither stabilized K → R mutant undergoes ubiquitination *in vivo*. As these lysines both face the cytosol, we had originally hypothesized that they might be ubiquitination sites, albeit quite distant along the primary sequence of Hmg2.

Interestingly, human HMGR similarly has two distant cytoplasmic lysines each required for regulated ERAD of the human form of the enzyme (22, 30).

We revisited these stabilizing mutations and tested each with the *in vitro* proteolysis assay to evaluate their ability to support GGPP-regulated misfolding. Despite not being a conserved SSD residue, K357R 1myc_L-Hmg2-GFP behaved
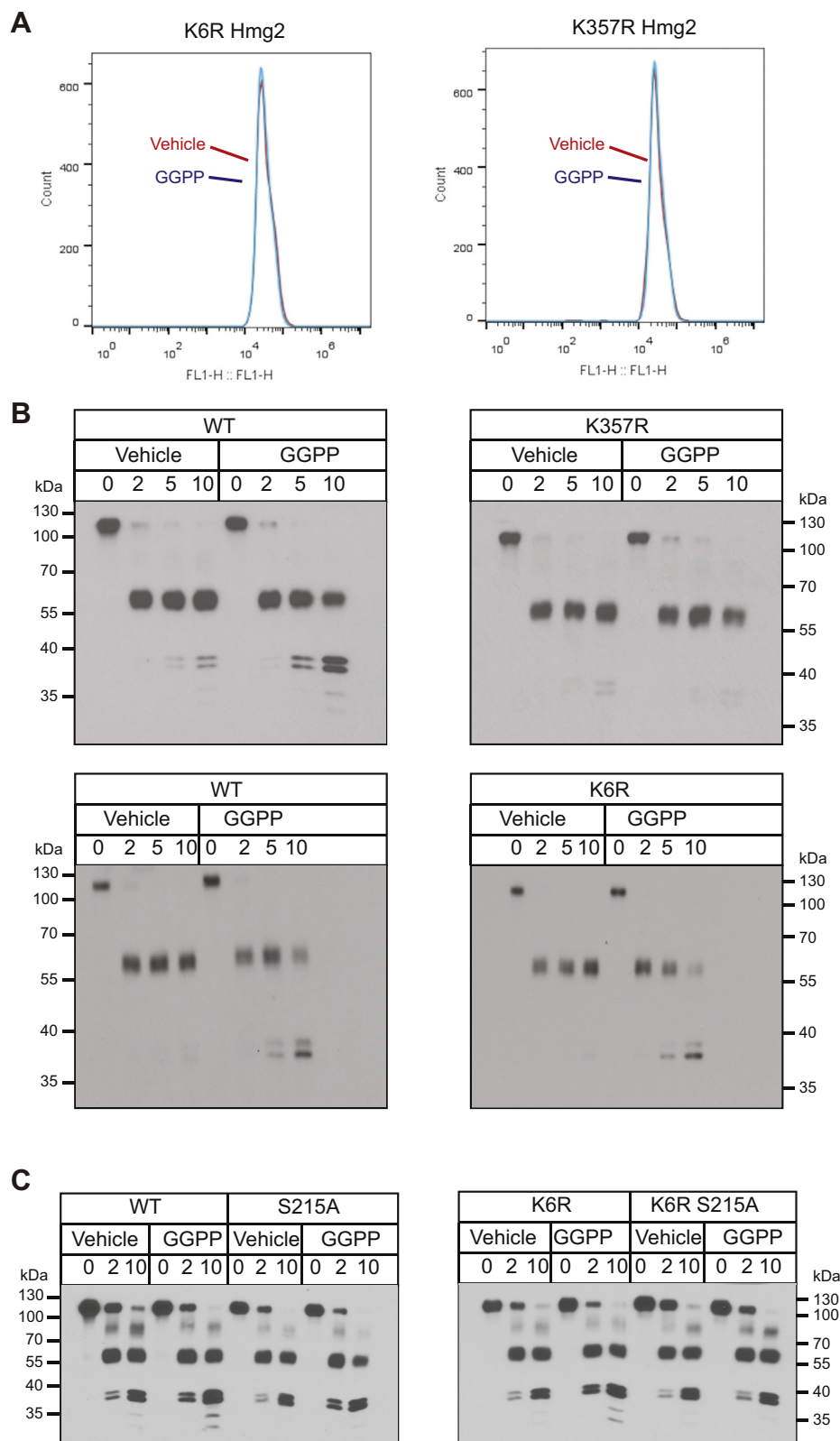
Figure 4. Separate sequence determinants of misfolding and degradation. *A*, the two lysine-to-arginine mutations, K6R and K357R each rendered Hmg2-GFP insensitive to the degradation signal GGPP. Strains expressing each mutant were treated with 22 μM GGPP (*blue curves*) for 2 h and then subjected to flow cytometry. Unlike wild-type Hmg2-GFP (Fig. 1*C*), GGPP did not affect K6R or K357R Hmg2-GFP levels compared with vehicle treatment (red curves). *B*, the mutation K357R blocked GGPP-induced misfolding *in vitro*, but the K6R mutation did not. Microsomes expressing wild-type, K357R, and K6R 1myc$_L$-Hmg2-GFP were isolated and treated with vehicle or 22 μM GGPP prior to proteolysis as in earlier figures. GGPP did not cause misfolding and increased proteolysis in the K357R mutant (top panels). Conversely, K6R 1myc$_L$-Hmg2-GFP responded to GGPP like the wild-type protein (bottom panels). *C*, in-cis epistasis of the K6R mutation and the SSD mutation S215A. Both wild-type and K6R 1myc$_L$-Hmg2-GFP misfolded upon 22 μM GGPP treatment, whereas the K6R S215A double mutation did not respond to GGPP treatment.

like the SSD mutants discussed above: it was completely unresponsive to added GGPP (Fig. 4*B*). Conversely, K6R 1myc$_L$-Hmg2-GFP, despite its extreme *in vivo* stability, showed an entirely normal response to GGPP, behaving identically to wild-type 1myc$_L$-Hmg2-GFP in the misfolding assay (Fig. 4*B*). This defined for the first time two classes of determinant for Hmg2 degradation and an apparent sequence of events: GGPP-dependent misfolding that was affected by SSD mutations such as S215A or K357R, followed by Hrd1-dependent ubiquitination that required K6, but after SSD-dependent misfolding. To test this idea, we performed a "cis-epigenetic" test of this model with double mutants from each class: the K6R mutant that allows regulated misfolding, and our strongest, best characterized SSD mutant—S215A—that fails to undergo regulated misfolding. Or model predicts that SSD-dependent misfolding occurs independently of ubiquitination: thus, we would expect the S215A mutant to abolish the GGPP response of the nonubiquitinated K6R mutant. That is what we observe: the K6R single mutant is still GGPP responsive, and this effect is lost in the double mutant, consistent with a model of GGPP-dependent misfolding that then triggers K6R-dependent degradation (Fig. 4*C*).

The SSD functions in the kinetics of GGPP-dependent Hmg2 misfolding

The above demonstrations of a separable, independent role of the SSD led us to more fully investigate the nature of the SSD's action in Hmg2 mallosteric misfolding. We wondered if the SSD was involved in determining the rate or extent of response to GGPP. Specifically, we examined whether Hmg2 with a strong stabilizing SSD mutation could still respond to GGPP at sufficiently high concentrations or long incubation times. We performed time course experiments testing wild-type or S215A 1myc$_L$-Hmg2-GFP in the *in vitro* proteolysis assay at a variety of GGPP concentrations and incubation times. Although the stable SSD mutants had not responded to GGPP in any of our normally conducted assays, we found that when incubated overnight with a high concentration of GGPP (approximately 1000 times that required for initial effects in the wild-type protein), S215A 1myc$_L$-Hmg2-GFP did indeed respond to GGPP (Fig. 5*A*). Despite the apparently much lower potency, the effect remained highly specific for GGPP: the previously described inactive analog 2F-GGPP was similarly unable to affect S215A Hmg2 in the extended time assay (Fig. 5*B*). A time course of GGPP incubation confirmed that the response time of S215A 1myc$_L$-Hmg2-GFP was severely delayed, with the mutant starting to respond to GGPP only after 2.5 h of treatment and with a maximal response occurring by 3.5 h (Fig. 5*C*). For comparison, wild-type 1myc-Hmg2-GFP responds to signal almost immediately, within less than 5 min when GGPP is added at the same time as protease.

"Toxic subunit" effects as a test of the Hmg2 multimer in mallostery

We had previously shown that the GGPP-mediated reversible misfolding of Hmg2 has many attributes of allosteric regulation (18). These include: high ligand potency and specificity, the existence of a specific GGPP antagonist, reversibility, and the biochemical observation that the Hmg2 transmembrane domain is a multimer *in vivo*. These similarities led us to suggest the name "mallostery" to describe GGPP-mediated misfolding of Hmg2. Nearly all cases of allosteric regulation involve structural changes based on concerted interaction between subunits of a regulated multimer. Accordingly, we wondered if the GGPP-mediated mallosteric misfolding would similarly depend on the observed multimeric structure of the Hmg2 transmembrane domain. The existence of the above-described mutants deficient in GGPP-mediated misfolding provided a powerful new experimental tool to test this feature of the mallosteric model. The idea is based on the observation of dominant negative mutations in many allosteric and cooperative proteins, in which the presence of a nonresponsive mutant subunit within an allosteric multimer can block the regulation of the whole multimeric assembly (38, 39). We hypothesized that the presence of a nonresponsive SSD mutant Hmg2 as a subunit of an Hmg2 multimer would interfere with GGPP-mediated response of the mixed quaternary structure. Conversely, we predicted that the K6R mutant that still undergoes GGPP-stimulated misfolding but is not ubiquitinated would still permit regulated degradation of its wild-type partners within a mixed multimer. To test this idea, we constructed yeast strains coexpressing both wild-type and nonresponsive SSD mutants, such that the behavior of the wild-type protein could be independently examined in the presence of a coexpressed mutant or wild-type control. Specifically, we coexpressed wild-type, optically detectable, normally regulated Hmg2-GFP along with nonfluorescent, nonresponsive S215A as well as testing control strains with a wild-type version of the nonfluorescent coexpressee. In this way we examined the behavior of only the normally regulated Hmg2-GFP by optical means when in the presence or absence of the coexpressed, nonfluorescent, nonresponsive mutants (Fig. 6*A*).

When these two versions of Hmg2 were coexpressed, the wild-type Hmg2-GFP coexpressed with S215A was degraded more slowly in a cycloheximide chase, implying that the coexpressed dark, S215A mutant stabilized the fluorescent wild-type Hmg2-GFP (Fig. 6*B*). Similarly, addition of GGPP to the strain coexpressing nonresponsive S215A-Hmg2 was much less effective at causing degradation of the wild-type Hmg2-GFP than in the otherwise identical strain coexpressing dark, wild-type Hmg2 (Fig. 6*C*).

We also tested for intersubunit interactions using the *in vitro* limited proteolysis assay. For these experiments, we used wild-type 1myc$_L$-Hmg2-GFP from the limited proteolysis experiments above, coexpressed with either wild-type or S215A Hmg2-GFP with no luminal myc tag, so that, in this assay as well, we could selectively observe—by myc immunoblotting—the proteolytic response of only 1myc$_L$-Hmg2-GFP in the presence of coexpressed but not-myc-tagged Hmg2 mutants (6D). We also included a strain expressing the single, highly stable protein S215A-1myc$_L$-Hmg2-GFP as a positive control to evaluate the strength of any trans effects observed. Again, we found that coexpression of the nonresponsive
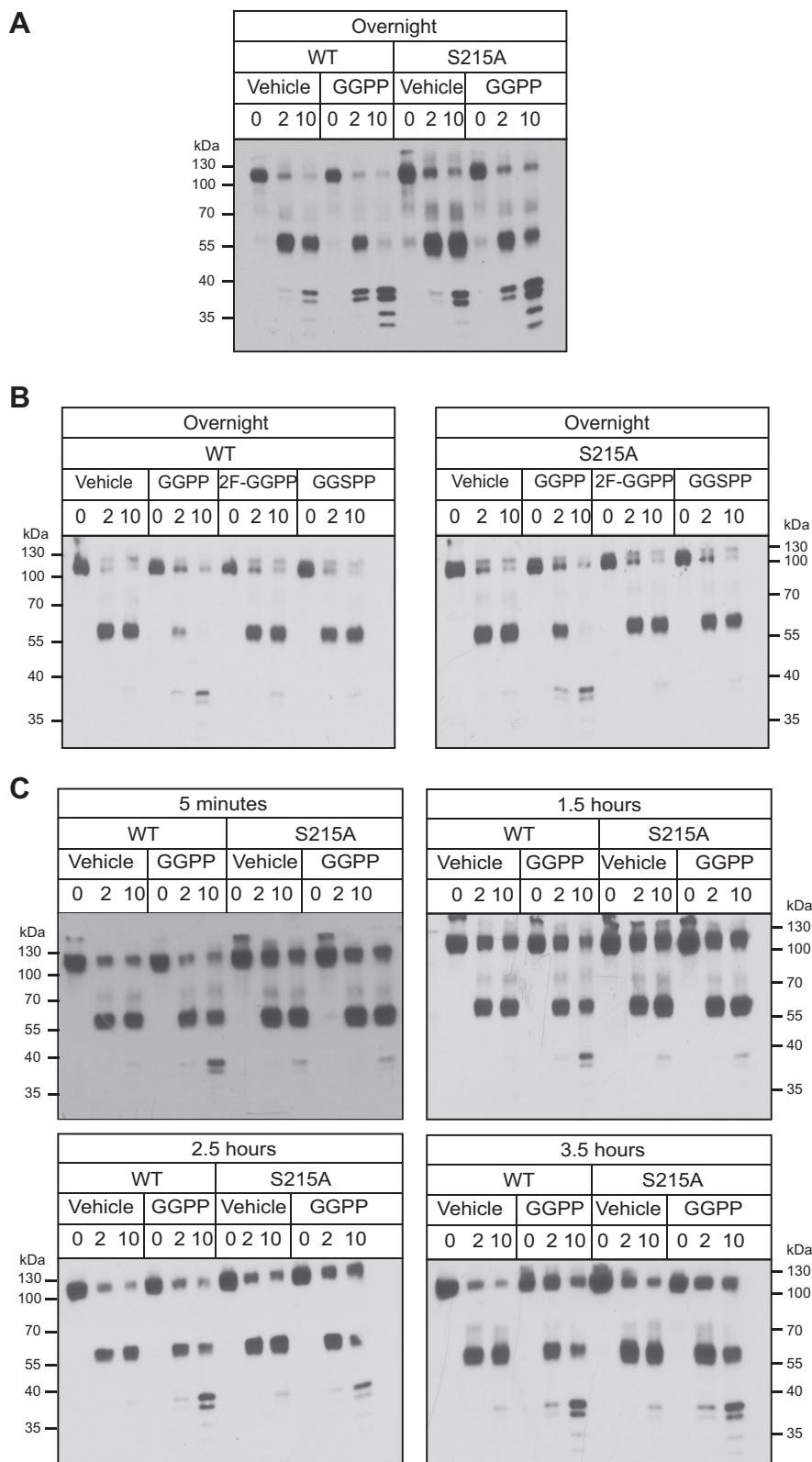
Figure 5. GGPP caused mallosteric misfolding of the stable SSD mutant S215A at high concentrations when treated for long time courses. *A*, overnight GGPP treatment caused *in vitro* misfolding of S215A Hmg2. Western blots of *in vitro* proteolysis performed on membranes from cells expressing wild-type or S215A 1mycL-Hmg2-GFP and incubated with vehicle or 22 μM GGPP overnight (15 h). *B*, GGPP-mediated, long time course misfolding of S215A maintained the high GGPP structural specificity observed in WT Hmg2. Specificity of overnight misfolding of wild-type or S215A 1mycL-Hmg2-GFP was tested by treatment with 22 μM of the close analogs of GGPP, 2-fluouro GGPP (2F-GGPP), and s-thiolo GGPP (GGSPP), shown to be inactive in more canonical rapid structural changes in wild-type Hmg2. Neither caused misfolding of either wild-type or S215A Hmg2 at the high concentrations and long time courses employed in this experiment. *C*, time course of wild-type and S215A GGPP-induced misfolding. Wild-type 1mycL-Hmg2-GFP misfolded in response to GGPP more quickly than can be measured, within 5 min. S215A 1mycL-Hmg2-GFP began to misfold in response to GGPP after approximately 2.5 h of treatment.
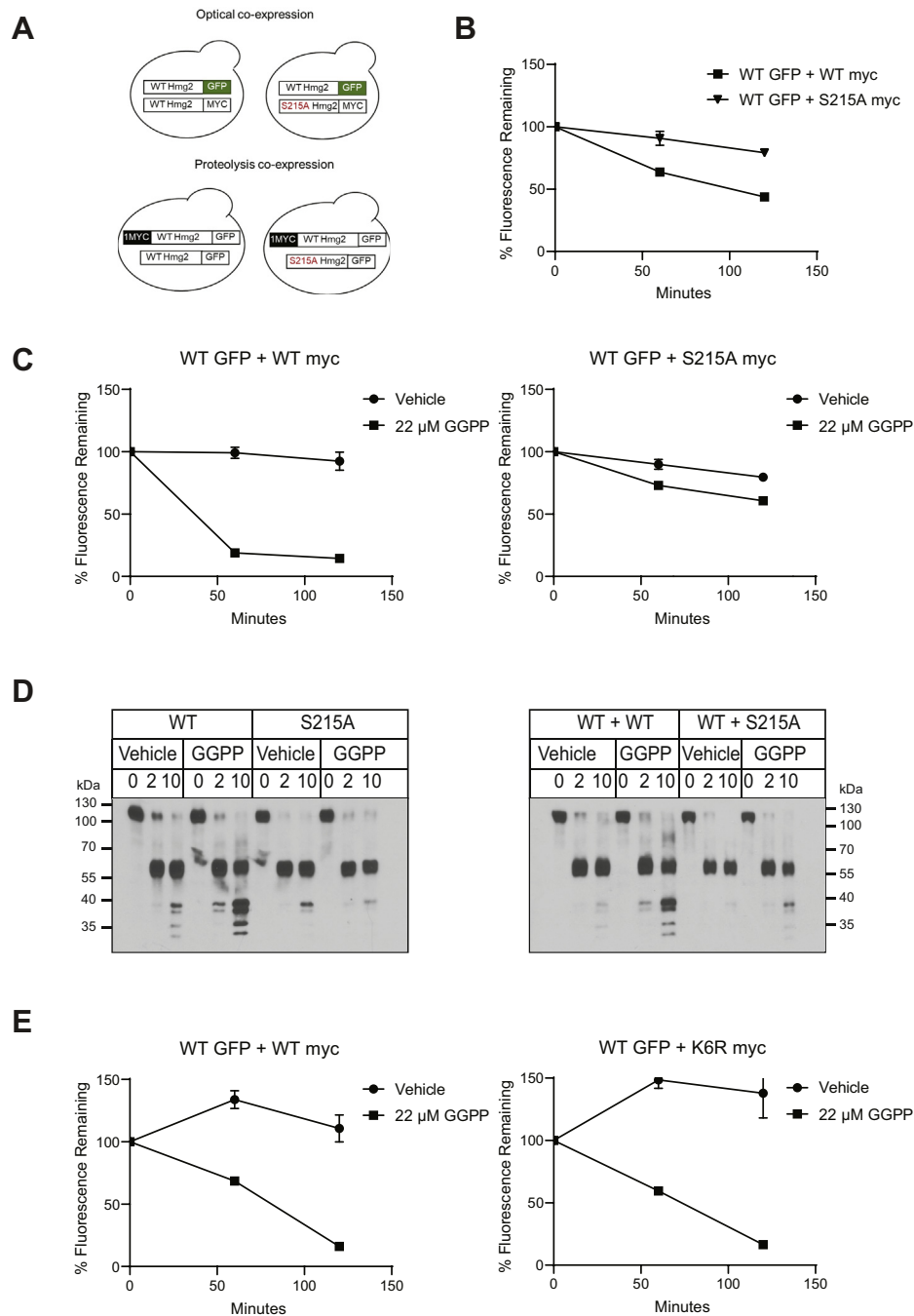
Figure 6. Trans effects of mutated SSDs on regulated misfolding. *A*, cartoon showing experimental setup for coexpression experiments. For optical experiments, WT Hmg2-GFP was coexpressed alongside a nonfluorescent, myc-tagged mutant S215A or WT (control) copy (top). For proteolysis experiments, WT 1myc$_L$-Hmg2-GFP was coexpressed alongside a GFP-tagged, without myc, mutant S215A Hmg2-GFP or WT (control) (bottom). *B*, coexpression of dark (nonfluorescent), myc-tagged, nonmallosteric mutant S215A Hmg2 strongly stabilized wild-type Hmg2-GFP. Wild-type Hmg2-GFP was expressed along with dark wild-type Hmg2-myc (*filled squares*) or S215A Hmg2-myc (*filled triangles*). In a cycloheximide chase, the dark S215A Hmg2-myc slowed the degradation of wild-type Hmg2-GFP when compared with a strain coexpressing wild-type Hmg2-myc. Error bars are SEM. *C*, coexpression of the dark S215A Hmg2-myc inhibited the response of wild-type Hmg2-GFP to GGPP. Wild-type Hmg2-GFP was coexpressed with wild-type Hmg2-myc (left) or S215A Hmg2-myc (right). Coexpression of the mutated Hmg2-myc, which cannot misfold, but not the wild-type Hmg2-myc, partially blocked GGPP-induced degradation of the wild-type Hmg2-GFP. *Filled circles* show vehicle control, and filled squares show GGPP treatment. Error bars are SEM. *D*, coexpression of a non-mallosteric SSD mutant Hmg2-GFP strongly blocked GGPP-induced misfolding of wild-type 1myc$_L$-Hmg2-GFP *in vitro*. Left, 22 µM GGPP induced misfolding and caused increased proteolytic cleavage in wild-type but not S215A 1myc$_L$-Hmg2-GFP. Right, coexpression of wild-type Hmg2-GFP without a myc tag did not interfere proteolysis of wild-type 1mycL-Hmg2-GFP. However, coexpression of S215A Hmg2-GFP with no myc tag attenuated GGPP-induced misfolding of the wild-type 1myc$_L$-Hmg2-GFP copy. *E*, coexpression of the highly stable but still mallosteric K6R Hmg2-myc allowed normal Hmg2-GFP regulation. Cells expressing Hmg2-GFP and coexpressing a dark wild-type Hmg2-myc (left) or K6R Hmg2-myc (right) were treated with vehicle (*filled circles*) or GGPP (*filled squares*), and Hmg2-GFP levels were assayed by flow cytometry. The K6R Hmg2-myc did not block regulation of the wild-type Hmg2-GFP. Error bars are SEM.

S215A Hmg2-GFP interfered with the ability of the wild-type copy to undergo GGPP-dependent misfolding (6D, right panel). Wild-type 1myc$_L$-Hmg2-GFP underwent normal *in vitro* misfolding in response to GGPP when the coexpressed, non-myc-tagged test protein was wild-type, but its response to GGPP was severely blunted when the coexpressed, nontagged protein had the S215A mutation (Fig. 6D). In fact, the stabilizing effect of coexpressing the S215A mutant on the also-present, wild-type 1myc$_L$-Hmg2-GFP was as strong as the stabilizing effect of the mutant in-cis—that is, when included in 1myc$_L$-S215A-Hmg2-GFP itself (compare 6D left (cis S215A effect) and right (coexpressed S215A effect) panels). Taken together, these *in vivo* and *in vitro* studies indicated that the mallosteric action of the SSD operates at the level of multimeric Hmg2, as indicated by the ability of nonresponsive SSD mutants to strongly affect the response of coexpressed but normal Hmg2 to the GGPP signal *in vivo* or *in vitro*.

The above coexpression tests of allosteric-style communication between subunits required for a "toxic subunit" effect are both powerful and classic, being borrowed from the deeply rooted literature of allosteric regulation (38, 39). Our model is that the regulated misfolding caused by an intact, wild-type SSD operates through the quaternary structure of the Hmg2 transmembrane region, and the presence of nonresponsive SSDs drastically affects the GGPP-mediated changes in structure of the multimer. However, other models could explain the interference of normal degradation caused by a coexpressed, highly stable version of Hmg2. For instance, perhaps introducing a highly stable coexpressed Hmg2 variant causes stabilization of Hmg2-GFP due to challenges to the capacity of the HRD degradation pathway. Accordingly, we ran a critical control coexpression test that further capitalized on the mutant analysis above. We tested whether the still-GGPP-responsive but highly stable K6R mutant had any effect when coexpressed with normally regulated Hmg2-GFP. The K6R mutant is also strongly stabilized like the S215A or K357R mutants, but underwent normal GGPP-mediated structural changes *in vitro* as shown above. Unlike the SSD mutants, coexpressing the highly stable K6R mutant had no effect on the degradation or the GGPP response of also-present Hmg2-GFP, indicating that the effect of the nonfunctional SSD mutants was specifically due to the loss of regulated misfolding within the coexpressed multimers (Fig. 6E).

Taken together, these studies strongly imply that the "mallosteric model" of GGPP causing reversible misfolding through concerted structural changes in the quaternary Hmg2 transmembrane domain is the mechanism of ligand-regulated Hmg2 misfolding.

GGPP-dependent mallostery was membrane-autonomous

Finally, we tested the ability of Hmg2 to undergo GGPP-dependent misfolding when removed from its normal membrane context after detergent solubilization. We prepared microsomes from the *in vitro* proteolysis strain expressing 1myc$_L$-Hmg2-GFP and subjected them to solubilization with a variety of detergents. Three of the detergents tested, Fos-Choline-13, Decyl Maltose Neopentyl Glycol (DMNG), and digitonin, yielded soluble 1myc$_L$-Hmg2-GFP that retained its normal pattern of proteolytic cleavage (Fig. 7A). This solubilized Hmg2 was, however, more sensitive to trypsin (data not shown), so lower concentrations of the protease were used in these experiments.

The preservation of the pattern of proteolysis was somewhat surprising, given that we had assumed that the luminal location of the 1myc$_L$ tag was required for protection from the added trypsin. These results imply that the luminal tag is further protected by some aspect of Hmg2 structure independent of luminal isolation. Whatever the cause of this "solution autonomy," the preservation of the myc-detected proteolysis pattern allowed us to examine the role of the mallosteric behavior of Hmg2 when completely separate from the ER membrane. Accordingly, we tested the response of detergent-solubilized 1myc$_L$-Hmg2-GFP to either chemical chaperones or GGPP using a soluble variant of the microsomal limited proteolysis assay. Solubilized 1myc$_L$-Hmg2-GFP appeared to be constitutively more structurally open than when present in the ER membrane, with high basal rates of proteolysis. However, it retained the ability to respond to the chemical chaperone glycerol in all three detergents: preparations treated with 20% glycerol were more resistant to proteolysis, as in the normal microsomal assay (Fig. 7, A–B). The GGPP-dependent structural response was more sensitive to choice of solubilization detergent. Hmg2-GFP solubilized with either Fos-Choline-13 or DMNG had no detectable response to GGPP, whether alone or in combination with glycerol treatment (Fig. 7A). Conversely, digitonin-solubilized preparations did indeed respond to GGPP in the limited proteolysis assay, although at higher concentrations than required in the original microsomal assay (Fig. 7A). Importantly, the non-responding stable S215A Hmg2 did not respond to GGPP in the digitonin-solubilized state (Fig. 7B), indicating that the SSD mediates the GGPP response in the micellar state in the absence of any membrane. Furthermore, the degree of response to GGPP in the digitonin-solubilized Hmg2 was lessened by coincubation with glycerol, as is the case in the microsomal assay as well as *in vivo*.

In the course of these studies, we also found that GGPP affected Hmg2 detergent solubility. After preparing and solubilizing microsomes, we added vehicle or GGPP to the preparations and further incubated for 1 h with gentle shaking. Afterward, we separated the samples by ultracentrifugation and found that preparations treated with GGPP had been more effectively solubilized by digitonin (Fig. 7C). The stable S215A Hmg2 did not become more solubilized by GGPP in these experiments (Fig. 7D). Furthermore, the inactive analog of GGPP, 2F-GGPP, which does not stimulate Hmg2 degradation *in vivo* or misfolding *in vitro*, did not have any effect on solubility in this assay (Fig. 7E), indicating that this effect is specific both to the structure of GGPP and to the misfolding capability of the SSD. Although these effects are small, it is intriguing that a straightforward, reproducible, and highly specific readout of the mallosteric response manifests at the level of protein biochemical behavior. Importantly, the change
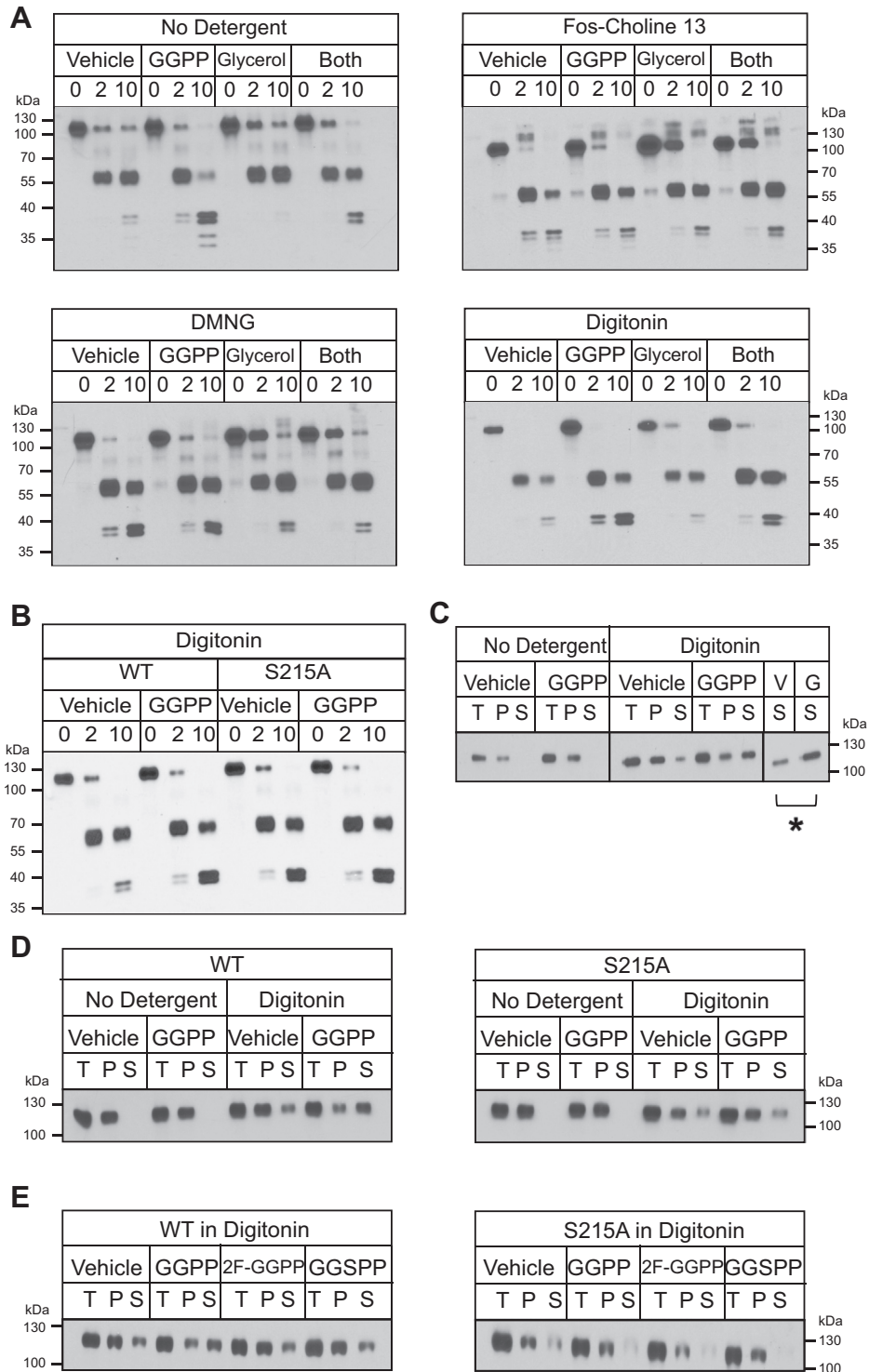
Figure 7. *In vitro* proteolysis assay of micellar 1myc$_L$-Hmg2-GFP is intact, and responses to glycerol and GGPP. *A*, the nonionic detergents fos-choline 13, decyl maltose neopentyl glycol (DMNG), and digitonin allowed the time-dependent proteolytic cleavage pattern of 1myc$_L$-Hmg2-GFP in solution. Microsomes from cells expressing 1myc$_L$-Hmg2-GFP were isolated as previously and left unsolubilized (top left) or subjected to solubilization with fos-choline 13 (top right), DMNG (bottom left), or digitonin (bottom right) as described in text. For the no detergent condition, the microsome pellet was used; for the three detergent conditions, solubilized microsomes were clarified by ultracentrifugation, and the supernatant was subjected to proteolysis. In fos-choline 13, DMNG, and digitonin, the 1myc$_L$-Hmg2-GFP myc tag remained intact during proteolysis. 1myc$_L$-Hmg2-GFP remained responsive to the action of the chemical chaperone glycerol in all three detergents. Furthermore, 1myc$_L$-Hmg2-GFP solubilized in digitonin remained responsive to GGPP *in vitro*. *B*, digitonin solubilization preserved the SSD requirement for 1myc$_L$-Hmg2-GFP misfolding. When solubilized with digitonin, proteolysis of wild-type 1myc$_L$-Hmg2-GFP increased in response to GGPP treatment, but proteolysis of S215A 1myc$_L$-Hmg2-GFP did not. *C*, GGPP treatment during solubilization increased the solubility of 1myc$_L$-Hmg2-GFP. Left, when not solubilized and subjected to centrifugation, 1myc$_L$-Hmg2-GFP was present only in the pellet when detected by western blotting for the myc tag. GGPP did not affect 1myc$_L$-Hmg2-GFP fractionation in unsolubilized microsomes. Right, when microsomes were solubilized with digitonin, 1myc$_L$-Hmg2-GFP was present in both pellet and supernatant fractions. Treatment of microsomes with 22 μM GGPP during solubilization increased the amount of 1myc$_L$-Hmg2-GFP in the supernatant fraction. Far right, comparison of the amount of 1myc$_L$-Hmg2-GFP

in ratio of soluble Hmg2 (S) to total Hmg2 (T) was statistically significant, as indicated by the bar in Figure 7C.

The whole of the above data indicate that the SSD is required for regulated misfolding and degradation of Hmg2. Lesions in the SSD block Hmg2 from responding to the degradation signal GGPP, preventing *in vivo* degradation and *in vitro* misfolding. The role of the SSD appears to be "kinetic," with long incubations at extremely high concentrations of signal eventually overcoming its loss. Hmg2 forms multimeric structures, and mutations in the SSD can block regulation in wild-type Hmg2 in-trans. The SSD constitutes a separate determinant for Hmg2-regulated misfolding, and its function is autonomous of INSIG proteins and partially retained even when removed from the normal context of the ER membrane.

Discussion

In this work we set out to understand structural features of Hmg2 that contribute to regulated degradation, with particular emphasis on role of the conserved SSD in the ligand-regulated misfolding that underlies mallostery. The SSD is a multi-spanning membrane motif found in a number of eukaryotic proteins involved in sterol synthesis, transport, and regulation. The demonstrated importance of the Hmg2 SSD in GGPP-mediated misfolding was consistent with a broad role of the SSD in mediating protein structural changes as a mechanism of metabolic regulation (13, 16, 40). Importantly, our results demonstrate an autonomous role for a bone fide SSD in protein regulation independent of the frequently described INSIG–SSD interactions often required for SSD actions. Furthermore, the genetic separability of regulated misfolding and HRD-dependent ubiquitination that capitalized on conserved SSD residues allowed us to test the mallosteric model of GGPP-regulated misfolding using coexpression studies. Taken together, these data indicate that ligand-mediated, regulatory misfolding can show precise and evolvable sequence underpinnings that bode well for both understanding the function of the SSD and opening the door for development of degradation-based therapeutic molecules for a variety of desired protein targets.

We tested highly conserved SSD residues for their role in regulated misfolding using both flow cytometry *in vivo* and a limited proteolysis assay of Hmg2 structure *in vitro*. Mutations in the SSD that stabilize Hmg2 *in vivo* also blocked GGPP-induced misfolding of Hmg2 *in vitro*, meaning that the proteolysis assay can serve as a biochemical test of SSD function. We had shown previously that all phenotypic SSD point mutations stabilize Hmg2 *in vivo*—no mutations of conserved residues resulted in decreased stability—suggesting that the normal function of SSD is to allow regulated misfolding to occur. Because of the near-universal involvement of INSIGs in the action of SSDs in cholesterol regulation (13, 29, 31–33), we tested whether the SSD-dependent structural change was intrinsic to the domain itself or rather required the yeast INSIG orthologs Nsg1 or Nsg2. Despite the expectation for an INSIG role, we found that neither INSIG paralog was required for SSD-dependent GGPP-regulated misfolding. However, consistent with our earlier studies (31, 32), coexpressing Nsg1 to levels matching Hmg2 actually blocked regulated *in vitro* misfolding and *in vivo* degradation. Hmg2 has been previously found to bind to INSIGs, but their role in yeast is an inhibitory one: yeast INSIGs blocks the ability of GGPP to promote Hmg2 degradation, and this interaction between Hmg2 and Nsg1 is lanosterol-dependent. The model put forth from those studies is that Hmg2 undergoes GGPP-regulated degradation and that INSIGs allow this only to occur when sterol synthesis (and thus lanosterol levels) is low and isoprenes such as GGPP would tend to accumulate (34). The data above are consistent with those previous studies, since *in vivo* regulation of Hmg2 by GGPP occurs in the absence of INSIG proteins, and the SSD-dependent regulation of Hmg2 is the core molecular feature of this regulation. This INSIG independence of SSD action establishes a clear, autonomous role for this conserved domain, which, in the case of Hmg2, is further regulated by INSIGs to impart a second layer of sterol pathway control.

It is worth noting that yeast Hmg2 occupies a particularly advantageous position for the study of SSDs and INSIGs. In most reported cases, either SSD action is totally dependent on INSIG proteins (SCAP; HMGR regulation) (33, 41–43) or completely independent of INSIGs (NPC1, *S. pombe* SCAP) (44, 45). Yeast Hmg2 regulation occupies a mechanistic "sweet spot" in which the SSD clearly functions autonomously to allow physiologically useful regulation by GGPP, but is modulated by sterol-dependent interaction with the endogenous INSIGs. Thus, questions of the independent and intertwined roles of these two key components of sterol biology, and how this interaction evolved, can be studied using the combined powers of yeast genetics, biochemistry, and molecular biology.

Using our limited proteolysis assay of GGPP action, we tested other, non-SSD Hmg2-stabilizing mutations. Our early work had identified mutations in a pair of cytoplasmic lysines, K6, located on the cytoplasmic N-terminus of Hmg2, and K357, located in its sixth cytoplasmic loop. Both K6R Hmg2 and K357R Hmg2 are extremely stable *in vivo*, both in a cycloheximide chase or upon treatment of cells with the misfolding signal GGPP (35). In addition, unlike wild-type Hmg2, neither mutated protein is detectably ubiquitinated in response to GGPP treatment. Accordingly, we tested these mutations in our *in vitro* misfolding assay. We found that whereas K357R Hmg2 did not respond to GGPP, K6R Hmg2 still underwent normal GGPP-dependent misfolding *in vitro*, in a manner identical to the wild-type protein. This was the first time we had identified separable Hmg2 sequence determinants required for misfolding *versus* ubiquitination and

---

in the supernatant when treated with vehicle *versus* GGPP. *$p \leq 0.05$. *D*, the solubilization effect of added GGPP was SSD-dependent. Left, treating preparations with GGPP during solubilization increased the amount of wild-type 1myc$_L$-Hmg2-GFP detectable in the supernatant. However, the solubility of S215A 1myc$_L$-Hmg2-GFP was not affected by GGPP. *E*, the increase in solubilization was specific for GGPP. Treating preparations with the close analogues of GGPP, 2-fluoro-GGPP (2F-GGPP), or s-thiolo GGPP (GGSPP) did not increase the amount of 1myc$_L$-Hmg2-GFP detectable in the supernatant.

degradation. Additionally, this result suggests a model wherein K6, as a cytosol-facing lysine, which prevents Hmg2 ubiquitination and degradation but not misfolding, may be a major or first ubiquitination site, while lysine 357 is instead (or in addition) required for regulated misfolding in response to GGPP. Indeed, studies with double mutants demonstrated that the still-misfolded yet stable K6R mutant showed the expected SSD dependency in its response to GGPP, indicating the autonomy of these two aspects of GGPP-regulated degradation.

The evidence for an autonomous role of the SSD and the separability of that role from ubiquitination and degradation led us to further explore the action of the SSD in GGPP-regulated misfolding. We found through extended time course experiments that the highly conserved SSD mutant S215A-Hmg2, which is extremely stable *in vivo* and *in vitro*, could indeed respond to GGPP, but only after long incubation times, with a response substantially delayed compared with that of the wild-type protein. Remarkably, the delayed response of the S215A mutant still showed the high structural specificity of the GGPP stimulus: the inactive GGPP analogues remained inactive in the long time course response of this stable variant. This indicates that the GGPP binding site may be distinct from a structure defined by the SSD, since the preservation of the strong structural specificity implies that the still-unknown GGPP binding site is intact. Clearly, the next step will have to be a combination of binding and structural studies to resolve this intriguing question.

We further explored the role of Hmg2's transmembrane region in the mallosteric response to the GGPP ligand by testing for trans effects in coexpression experiments. In light of the demonstrable role for the SSD in the effect of GGPP, and the fact that the Hmg2 transmembrane region exists as a multimer, we asked if the presence of subunits with nonresponsive SSD mutations could affect the regulation of a wild-type Hmg2 within the same multimer through interactions typical of allostery. Specifically, we coexpressed mutant and wild-type SSDs in the same cells and measured the effect of the lesioned domain on the coexpressed wild-type domain's ability to undergo GGPP-dependent misfolding and degradation. Indeed, we found that a nonresponsive SSD is able to interfere with the action of the wild-type protein in trans. Importantly, an equally coexpressed K6R mutant, which is similarly stable but has a normal SSD-dependent response to GGPP, did not interfere with wild-type regulation. This sort of "poisoned subunit" experiment provides further evidence for SSD-mediated regulation of the Hmg2 folding state based on the mallosteric model. These coexpression experiments suggest a model for Hmg2 misfolding wherein the transmembrane domains of multimeric Hmg2 must cooperate to undergo concerted, multisubunit-based GGPP-regulated structural changes, which might be expected for the development of mallosteric regulation as a variation of cooperativity and allostery.

The above findings suggest a model for the SSD as an autonomous module for promoting misfolding in response to a regulatory ligand. By this model, GGPP binding at an unknown Hmg2 site causes the SSD to undergo a conformational change that renders the protein more susceptible to the HRD

quality control pathway. Lesions in the SSD block this change at physiologically relevant concentrations and timescales. This role for the SSD appears to be a kinetic one, as mutations in the SSD do not appear to block the conformational change absolutely, nor the high specificity of the GGPP ligand, so much as rendering it impractically slow for cellular regulation.

The mallosteric model for SSD action leaves several open questions, first and foremost, what is the mechanistic role of the SSD? Is the SSD executing a structural transition between a folded and "misfolded" state in response to the misfolding signal GGPP, or alternatively, is the SSD responsible for GGPP binding? Our current *in vitro* approaches do not definitively distinguish between mutations in Hmg2 that eliminate GGPP binding and those that allow binding but disable misfolding in response to binding elsewhere. Our time course experiments showing that a mutated SSD can still specifically respond to GGPP, albeit over the course of several hours rather than seconds, suggest that the SSD may play a role in allowing rapid transition between a folded and misfolded state, rather than mediating binding per se. The idea that SSD mediates structural changes in response to binding at a distinct site has arisen in studies of SCAP, which responds to sterols that bind to the first luminal loop of the protein by an SSD-dependent structural change (46, 47). Intriguingly, sequence and structural homology to SCAP and small regions of GGPP binding proteins suggest a similar distinct GGPP binding site, although direct tests have not yet been performed.

Alternatively, there are also studies indicating that SSDs can directly interact with ligands and thus allow the possibility that it is the GGPP binding site (48–52). The SSD is related to the Resistance Nodulation Division (RND) domain, which is conserved in all domains of life and found in many transporters (53–56). Indeed, recent structures of the SSD of NPC1 suggest that in that protein the SSD functions in transport of sterol-related molecules and have located a putative sterol-interacting pocket within the domain (51), lending credence to the alternate possibility of the SSD as the GGPP binding site. Clearly further studies are required to resolve the divergent mechanistic underpinning of the mallosteric regulation of Hmg2 ERAD.

In the course of this work, we also extended our analysis of GGPP-mediated misfolding to detergent-solubilized Hmg2. We wondered if solubilized $1myc_L$-Hmg2-GFP would still show a useful proteolytic pattern in the absence of a protected luminal space and, given that, if detergent-solubilized protein would remain responsive to chemical chaperones and/or GGPP. Remarkably, we found that all three of these responses could be true for Hmg2 in solution: the overall proteolytic pattern of Hmg2 in the *in vitro* misfolding assay was preserved when solubilized in several weak detergents, and Hmg2 in detergent solution retained the ability to be chaperoned by glycerol. Furthermore, in digitonin, Hmg2 retained its ability to undergo GGPP-mediated misfolding, with a preserved requirement for an intact SSD and the same high structural dependence on the GGPP molecule. The ability of solubilized Hmg2 to undergo ligand-regulated structural changes heralds

a new collection of approaches that could resolve nearly all of the structural and functional questions put forth above about the molecular functions of the SSD and its role in mallosteric regulation of Hmg2.

The SSD is conserved in a variety of proteins from yeast to humans (13, 23, 56–61), many of them implicated in human diseases, ranging from dyslipidemia, which affects nearly half of American adults and a quarter of American youths in some fashion (62, 63), to inborn genetic disorders (64, 65), to cancer (66). The human homolog of Hmg2, HMGR, as well as the SSD-containing SCAP, are both critical components of sterol biosynthesis and regulation, and human HMGR is the target of the cholesterol-lowering statin class of drugs. Another SSD-containing protein, NPC1-Like Protein 1 (NPC1L1) is involved in enteric cholesterol transport and targeted by the cholesterol-lowing drug ezetimibe (67, 68). Furthermore, three proteins associated with human inborn diseases, 7-dehydrocholesterol reductase (DHCR7), lesions in which cause Smith–Lemli–Opitz Syndrome (69–71), NPC1, lesions in which cause Niemann Pick Disease Type C (72, 73), and Patched, a regulator of Hedgehog signaling associated with the human cancer disorder Gorlin Syndrome (66, 74), all contain SSDs. In many proteins in which the role of the SSD is well understood, the motif seems to allow molecular outcomes related to protein quality control, ranging from entry into the ERAD pathway, as in both *S. cerevisiae* Hmg2 and human HMGR, and a control point between ER retention and engaging the ER–Golgi trafficking machinery, as in human SCAP and the *S. pombe* analogue Scp1 (13). The involvement of the SSD in a range of pressing human health issues makes it an intriguing target for further studies of regulated misfolding and proteostasis. More broadly, the phenomenon of small-molecule-mediated misfolding represents another potential tool for pharmaceutical intervention. In its broadest application, this mallosteric strategy holds untapped potential for targeting proteins less amenable to traditional active site drugs by instead targeting them for either stabilization or for misfolding and degradation.

Experimental procedures

Reagents

Geranylgeranyl pyrophosphate (GGPP), cycloheximide, trypsin, and digitonin were purchased from Sigma-Aldrich. Digitonin was washed and recrystallized in ethanol three times according to the manufacturer's instructions. Lovastatin was a gift from Merck & Co (Rahway NJ). GGSPP and 2-fluoro-GGPP were gifts from Reuben Peters (Iowa State University) and Philip Zerbe (University of California Davis). Fos-Choline-13 and Decyl Maltose Neopentyl Glycol were purchased from Anatrace. Anti-myc 9E10 supernatant was prepared from cells (CRL 1729, American Type Culture Collection) cultured in RPMI1640 medium (GIBCO BRL) with 10% fetal calf serum. Living colors mouse anti-GFP monoclonal antibody was purchased from Clontech, and HRP-conjugated goat antimouse antibody was purchased from Jackson ImmunoResearch.

Strains and plasmids

Yeast strains (Table S1) and plasmids (Table S2) were made by standard techniques. Yeast strains were isogenic and were made from the S288C background. Yeasts were grown in rich media (YPD) or in minimal media (Diffco Yeast Nitrogen Base with required amino acids and nucleic acids and 2% glucose) at 30 °C.

Hmg2 mutation plasmids were made by splicing by overlap extension (SOEing) or site-directed mutagenesis using the Life Technologies GeneArt system.

Ura3 Hmg2-GFP, $1myc_L$-Hmg2-GFP, and Hmg2-1myc plasmids were introduced at the *ura3-52* locus by integration of plasmid cut with *StuI*. Leu2 Hmg2-GFP plasmids were introduced into the promoter of the *leu2Δ* locus by integration of plasmid cut with *PpuMI*.

Flow cytometry

Flow cytometry experiments were performed as previously described (28). Yeast cultures were grown in minimal media to early log phase. Indicated molecules (22 μM GGPP or 50 μg/ml cycloheximide) or equal volumes of vehicle (7:3 methanol: 10 mM ammonium bicarbonate for GGPP and DMSO for cycloheximide) were added directly to culture medium. Cell fluorescence was measured for 10,000 cells per condition using a BD Accuri C6 flow cytometer (BD Biosciences). Flow data were analyzed using FlowJo software (FlowJo, LLC). Any averages shown are means of 10,000 ungated events.

Microsome preparation

Microsomes were prepared as described previously (27, 34). Yeasts were grown to mid log phase in YPD, and 10 OD equivalents were pelleted, washed in water, and resuspended in 240 μl lysis buffer (0.24 M sorbitol, 1 mM EDTA, 20 mM KH_2PO_4/K_2HPO_4, pH 7.5) with PIs (2 mM phenylmethylsulfonyl fluoride and 142 mM tosylphenylalanyl chloromethyl ketone). Acid-washed glass beads were added up to the meniscus. Cells were lysed on a multivortexer at 4 °C for six to eight 1-min intervals with 1 min on ice in between each lysis step. The lysates were transferred to a new tube, and lysates cleared with 5-s pulses of centrifugation. Microsomes were pelleted from cleared lysates by centrifugation at 14,000g for 5 min. Microsome pellets were washed once in XL buffer (1.2 M sorbitol, 5 mM EDTA, 0.1 M KH_2PO_4/K_2HPO_4, pH 7.5) and resuspended in XL buffer for limited proteolysis.

Limited proteolysis assay

The limited proteolysis assay was performed as described previously (Shearer & Hampton 2004). Microsomes in XL buffer were treated with the indicated isoprenoid molecules or with equal volumes of vehicle controls. For the S215A kinetic experiments, microsomes were preincubated with isoprenoids or vehicle for the indicated times. In all other cases, isoprenoids were added and then samples were immediately incubated at 30 °C with 15 μg/ml trypsin. Samples were quenched at the indicated times with equal volumes of 2× urea sample buffer (USB; 8 M urea, 4% SDS, 1 mM DTT, 125 mM Tris base, pH 6.8) and incubated at 55 °C for 10 min. Samples

Detergent limited proteolysis assay

The limited proteolysis assay was performed as described above with the following variations: After initial pelleting and washing of microsomes, microsomes were first thoroughly resuspended in XL buffer and then solubilized by the addition of detergent solution at10x the desired final concentration in XL buffer (final concentration 0.1% Fos-Choline-13, 0.05% DMNG, 0.5% or 1% digitonin). Preparations with detergent were incubated at 4 °C for 1 h with rocking and then repeatedly pipetted up and down. Finally, samples were cleared by centrifugation in a benchtop microcentrifuge for 15 min at 16,000g. The supernatants were then separated by ultracentrifugation at 89,000 RPM for 15 min, and the supernatant from this step was used for the proteolytic assay. This assay was identical to the limited proteolysis assay described above, except that a lower concentration of trypsin (3 μg/ml instead of 15) was used.

Detergent solubility assay

Microsomes were prepared as in the detergent limited proteolysis assay up to the point of detergent addition. After thorough mixing, 22 μl of GGPP, 2F-GGPP, GGSPP, or equal volume of vehicle was added as indicated. Microsomes were then incubated at 4 °C for 1 h with rocking. Samples were again pipetted vigorously up and down and then were separated by ultracentrifugation at 89,000 RPM for 15 min. Pellet and supernatant were separated and incubated in USB for 10 min at 55 °C and then resolved and immunoblotted as described above.

Data availability

All data are included within the manuscript. Raw data are available upon request. Additional information on reagents is presented in the supplemental information.

Conflict of interest—The authors declare that they have no conflicts of interest with the contents of this article.

Dedications—The authors wish to dedicate this manuscript to the memory of Dr Robert Simoni, who passed away during the review process. Bob was a major early inspiration for all lines of inquiry in the Hampton Lab, a constant encouraging colleague, and a true force generator for modern publication practices. Bob's creativity, enthusiasm, vision, scholarship, and volcanic laugh will all be sorely missed.

Abbreviations—The abbreviations used are: DMNG, decyl maltose neopentyl glycol; ERAD, endoplasmic-reticulum-associated protein degradation; GGPP, geranylgeranyl pyrophosphate; HMGR, HMG-CoA reductase; INSIGs, insulin-stimulated genes; RND, resistance nodulation division; SSD, sterol sensing domain; USB, urea sample buffer.

References

1. Needham, P. G., and Brodsky, J. L. (2013) How early studies on secreted and membrane protein quality control gave rise to the ER associated degradation (ERAD) pathway: the early history of ERAD. *Biochim. Biophys. Acta.* **1833**, 2447–2457
2. Mehnert, M., Sommer, T., and Jarosch, E. (2010) ERAD ubiquitin ligases. *BioEssays* **32**, 905–913
3. Smith, M. H., Ploegh, H. L., and Weissman, J. S. (2011) Road to ruin: targeting proteins for degradation in the endoplasmic reticulum. *Science* **334**, 1086–1090
4. Mehrtash, A. B., and Hochstrasser, M. (2019) Ubiquitin-dependent protein degradation at the endoplasmic reticulum and nuclear envelope. *Semin. Cell Dev. Biol.* **93**, 111–124
5. Hampton, R. Y., and Rine, J. (1994) Regulated degradation of HMG-CoA reductase, an integral membrane protein of the endoplasmic reticulum, in yeast. *J. Cell Biol.* **125**, 299–312
6. Hampton, R. Y., Gardner, R. G., and Rine, J. (1996) Role of 26S proteasome and HRD genes in the degradation of 3-hydroxy-3-methylglutaryl-CoA reductase, an integral endoplasmic reticulum membrane protein. *Mol. Biol. Cell.* **7**, 2029–2044
7. Gardner, R. G., Shearer, A. G., and Hampton, R. Y. (2001) *In vivo* action of the HRD ubiquitin ligase complex: mechanisms of endoplasmic reticulum quality control and sterol regulation. *Mol. Cell. Biol.* **21**, 4276–4291
8. Schumacher, M. M., Elsabrouty, R., Seemann, J., Jo, Y., and DeBose-Boyd, R. A. (2015) The prenyltransferase UBIAD1 is the target of geranylgeraniol in degradation of HMG CoA reductase. *Elife* **4**, e05560
9. Song, B.-L., Sever, N., and DeBose-Boyd, R. A. (2005) Gp78, a membrane-anchored ubiquitin ligase, associates with insig-1 and couples sterol-regulated ubiquitination to degradation of HMG CoA reductase. *Mol. Cell.* **19**, 829–840
10. Menzies, S. A., Volkmar, N., van den Boomen, D. J. H., Timms, R. T., Dickson, A. S., Nathan, J. A., and Lehner, P. J. (2018) The sterol-responsive RNF145 E3 ubiquitin ligase mediates the degradation of HMG-CoA reductase together with gp78 and hrd1. *Elife* **7**, e40009
11. Fuhrer, F., Langklotz, S., and Narberhaus, F. (2006) The C-terminal end of LpxC is required for degradation by the FtsH protease. *Mol. Microbiol.* **59**, 1025–1036
12. Wojcikiewicz, R. J., Furuichi, T., Nakade, S., Mikoshiba, K., and Nahorski, S. R. (1994) Muscarinic receptor activation down-regulates the type I inositol 1,4,5-trisphosphate receptor by accelerating its degradation. *J. Biol. Chem.* **269**, 7963–7969
13. Wangeline, M. A., Vashistha, N., and Hampton, R. Y. (2017) Proteostatic tactics in the strategy of sterol regulation. *Annu. Rev. Cell Dev. Biol.* **33**, 467–489
14. Stevenson, J., Luu, W., Kristiana, I., and Brown, A. J. (2014) Squalene mono-oxygenase, a key enzyme in cholesterol synthesis, is stabilized by unsaturated fatty acids. *Biochem. J.* **461**, 435–442
15. Foresti, O., Ruggiano, A., Hannibal-Bach, H. K., Ejsing, C. S., and Carvalho, P. (2013) Sterol homeostasis requires regulated degradation of

squalene monooxygenase by the ubiquitin ligase Doa10/Teb4. *Elife* **2**, e00953

16. Sharpe, L. J., Cook, E. C. L., Zelcer, N., and Brown, A. J. (2014) The UPS and downs of cholesterol homeostasis. *Trends Biochem. Sci.* **39**, 527–535

17. Garza, R. M., Tran, P. N., and Hampton, R. Y. (2009) Geranylgeranyl pyrophosphate is a potent regulator of HRD-dependent 3-Hydroxy-3-methylglutaryl-CoA reductase degradation in yeast. *J. Biol. Chem.* **284**, 35368–35380

18. Wangeline, M. A., and Hampton, R. Y. (2018) "Mallostery"—ligand-dependent protein misfolding enables physiological regulation by ERAD. *J. Biol. Chem.* **293**, 14937–14950

19. Theesfeld, C. L., Pourmand, D., Davis, T., Garza, R. M., and Hampton, R. Y. (2011) The sterol-sensing domain (SSD) directly mediates signal-regulated endoplasmic reticulum-associated degradation (ERAD) of 3-hydroxy-3-methylglutaryl (HMG)-CoA reductase isozyme Hmg2. *J. Biol. Chem.* **286**, 26298–26307

20. Millard, E. E., Gale, S. E., Dudley, N., Zhang, J., Schaffer, J. E., and Ory, D. S. (2005) The sterol-sensing domain of the Niemann-Pick C1 (NPC1) protein regulates trafficking of low density lipoprotein cholesterol. *J. Biol. Chem.* **280**, 28581–28590

21. Raychaudhuri, S., Young, B. P., Espenshade, P. J., and Loewen, C. J. (2012) Regulation of lipid metabolism: a tale of two yeasts. *Curr. Opin. Cell Biol.* **24**, 502–508

22. Jo, Y., and DeBose-Boyd, R. A. (2010) Control of cholesterol synthesis through regulated ER-associated degradation of HMG CoA reductase. *Crit. Rev. Biochem. Mol. Biol.* **45**, 185–198

23. Yabe, D., Xia, Z.-P., Adams, C. M., and Rawson, R. B. (2002) Three mutations in sterol-sensing domain of SCAP block interaction with insig and render SREBP cleavage insensitive to sterols. *Proc. Natl. Acad. Sci. U. S. A.* **99**, 16672–16677

24. Hughes, A. L., Stewart, E. V., and Espenshade, P. J. (2008) Identification of twenty-three mutations in fission yeast Scap that constitutively activate SREBP. *J. Lipid Res.* **49**, 2001–2012

25. Garza, R. M., Tran, P. N., and Hampton, R. Y. (2009) Geranylgeranyl pyrophosphate is a potent regulator of HRD-dependent 3-Hydroxy-3-methylglutaryl-CoA reductase degradation in yeast. *J. Biol. Chem.* **284**, 35368–35380

26. Gardner, R. G., and Hampton, R. Y. (1999) A highly conserved signal controls degradation of 3-hydroxy-3-methylglutaryl-coenzyme A (HMG-CoA) reductase in eukaryotes. *J. Biol. Chem.* **274**, 31671–31678

27. Shearer, A. G., and Hampton, R. Y. (2004) Structural control of endoplasmic reticulum-associated degradation: effect of chemical chaperones on 3-hydroxy-3-methylglutaryl-CoA reductase. *J. Biol. Chem.* **279**, 188–196

28. Shearer, A. G., and Hampton, R. Y. (2005) Lipid-mediated, reversible misfolding of a sterol-sensing domain protein. *EMBO J.* **24**, 149–159

29. Sever, N., Yang, T., Brown, M. S., Goldstein, J. L., and DeBose-Boyd, R. A. (2003) Accelerated degradation of HMG CoA reductase mediated by binding of insig-1 to its sterol-sensing domain. *Mol. Cell.* **11**, 25–33

30. Sever, N., Song, B.-L., Yabe, D., Goldstein, J. L., Brown, M. S., and DeBose-Boyd, R. A. (2003) Insig-dependent ubiquitination and degradation of mammalian 3-Hydroxy-3-methylglutaryl-CoA reductase stimulated by sterols and geranylgeraniol. *J. Biol. Chem.* **278**, 52479–52490

31. Flury, I., Garza, R., Shearer, A., Rosen, J., Cronin, S., and Hampton, R. Y. (2005) INSIG: a broadly conserved transmembrane chaperone for sterol-sensing domain proteins. *EMBO J.* **24**, 3917–3926

32. Theesfeld, C. L., and Hampton, R. Y. (2013) Insulin-induced gene protein (INSIG)-dependent sterol regulation of Hmg2 endoplasmic reticulum-associated degradation (ERAD) in yeast. *J. Biol. Chem.* **288**, 8519–8530

33. Yang, T., Espenshade, P. J., Wright, M. E., Yabe, D., Gong, Y., Aebersold, R., Goldstein, J. L., and Brown, M. S. (2002) Crucial step in cholesterol homeostasis: sterols promote binding of SCAP to INSIG-1, a membrane protein that facilitates retention of SREBPs in ER. *Cell* **110**, 489–500

34. Theesfeld, C. L., and Hampton, R. Y. (2013) Insulin-induced gene protein (INSIG)-dependent sterol regulation of Hmg2 endoplasmic reticulum-associated degradation (ERAD) in yeast. *J. Biol. Chem.* **288**, 8519–8530

35. Gardner, R., Cronin, S., Leader, B., Rine, J., Hampton, R., and Leder, B. (1998) Sequence determinants for regulated degradation of yeast

36. Gardner, R. G., and Hampton, R. Y. (1999) A "distributed degron" allows regulated entry into the ER degradation pathway. *EMBO J.* **18**, 5994–6004

37. Gardner, R. G., Shan, H., Matsuda, S. P., and Hampton, R. Y. (2001) An oxysterol-derived positive signal for 3-hydroxy- 3-methylglutaryl-CoA reductase degradation in yeast. *J. Biol. Chem.* **276**, 8681–8694

38. Betz, J. L., and Fall, M. Z. (1988) Effects of dominant-negative lac repressor mutations on operator specificity and protein stability. *Gene* **67**, 147–158

39. Eisensteins, E., Hang, M. S., Wooll, T. S., Ritcheyll, J. M., Gibbons, I., Yang, Y. R., and Schachmanss, H. K. (1992) Negative complementation in aspartate transcarbamylase analysis of hybrid enzyme molecules containing different arrangements of polypeptide chains from wild-type and inactive mutant catalytic subunits. *J. Biol. Chem.* **267**, 22148–22155

40. Espenshade, P. J., and Hughes, A. L. (2007) Regulation of sterol synthesis in eukaryotes. *Annu. Rev. Genet.* **41**, 401–427

41. Song, B.-L., Javitt, N. B., and DeBose-Boyd, R. A. (2005) Insig-mediated degradation of HMG CoA reductase stimulated by lanosterol, an intermediate in the synthesis of cholesterol. *Cell Metab.* **1**, 179–189

42. Radhakrishnan, A., Goldstein, J. L., McDonald, J. G., and Brown, M. S. (2008) Switch-like control of SREBP-2 transport triggered by small changes in ER cholesterol: a delicate balance. *Cell Metab.* **8**, 512–521

43. Jo, Y., Lee, P. C. W., Sguigna, P. V., and DeBose-Boyd, R. A. (2011) Sterol-induced degradation of HMG CoA reductase depends on interplay of two Insigs and two ubiquitin ligases, gp78 and Trc8. *Proc. Natl. Acad. Sci. U. S. A.* **108**, 20503–20508

44. Schultz, M. L., Krus, K. L., and Lieberman, A. P. (2016) Lysosome and endoplasmic reticulum quality control pathways in Niemann-Pick type C disease. *Brain Res.* **1649**, 181–188

45. Hughes, A. L., Todd, B. L., and Espenshade, P. J. (2005) SREBP pathway responds to sterols and functions as an oxygen sensor in fission yeast. *Cell* **120**, 831–842

46. Motamed, M., Zhang, Y., Wang, M. L., Seemann, J., Kwon, H. J., Goldstein, J. L., and Brown, M. S. (2011) Identification of luminal loop 1 of scap protein as the sterol sensor that maintains cholesterol homeostasis. *J. Biol. Chem.* **286**, 18002–18012

47. Gao, Y., Zhou, Y., Goldstein, J. L., Brown, M. S., and Radhakrishnan, A. (2017) Cholesterol-induced conformational changes in the sterolsensing domain of the Scap protein suggest feedback mechanism to control cholesterol synthesis. *J. Biol. Chem.* **292**, 8729–8737

48. Li, X., Wang, J., Coutavas, E., Shi, H., Hao, Q., and Blobel, G. (2016) Structure of human Niemann–Pick C1 protein. *Proc. Natl. Acad. Sci. U. S. A.* **113**, 8212–8217

49. Gong, X., Qian, H., Zhou, X., Wu, J., Wan, T., Cao, P., Huang, W., Zhao, X., Wang, X., Wang, P., Shi, Y., Gao, G. F., Zhou, Q., and Yan, N. (2016) Structural insights into the Niemann-Pick C1 (NPC1)-mediated cholesterol transfer and ebola infection. *Cell* **165**, 1467–1478

50. Kwon, H. J., Abi-Mosleh, L., Wang, M. L., Deisenhofer, J., Goldstein, J. L., Brown, M. S., and Infante, R. E. (2009) Structure of N-terminal domain of NPC1 reveals distinct subdomains for binding and transfer of cholesterol. *Cell* **137**, 1213–1224

51. Davies, J. P., and Ioannou, Y. A. (2000) Topological analysis of Niemann-Pick C1 protein reveals that the membrane orientation of the putative sterol-sensing domain is identical to those of 3-hydroxy-3-methylglutaryl-CoA reductase and sterol regulatory element binding protein cleavage-activating protein. *J. Biol. Chem.* **275**, 24367–24374

52. Zhang, Y., Bulkley, D. P., Xin, Y., Roberts, K. J., Asarnow, D. E., Sharma, A., Myers, B. R., Cho, W., Cheng, Y., and Beachy, P. A. (2018) Structural basis for cholesterol transport-like activity of the Hedgehog receptor patched. *Cell* **175**, 1352–1364.e14

53. Roberg-Larsen, H., Strand, M. F., Krauss, S., and Wilson, S. R. (2014) Metabolites in vertebrate Hedgehog signaling. *Biochem. Biophys. Res. Commun.* **446**, 669–674

54. Nikaido, H., and Takatsuka, Y. (2009) Mechanisms of RND multidrug efflux pumps. *Biochim. Biophys. Acta.* **1794**, 769–781

55. Hausmann, G., von Mering, C., and Basler, K. (2009) The Hedgehog signaling pathway: where did it come from? *PLoS Biol.* **7**, e1000146

ASBMB

56. Osborne, T. F., and Espenshade, P. J. (2009) Evolutionary conservation and adaptation in the mechanism that regulates SREBP action: what a long, strange tRIP it's been. *Genes Dev.* **446**, 669–674

57. Osborne, T. F., and Rosenfeld, J. M. (1998) Related membrane domains in proteins of sterol sensing and cell signaling provide a glimpse of treasures still buried within the dynamic realm of intracellular metabolic regulation. *Curr. Opin. Lipidol.* **9**, 137–140

58. Zhong, Y., Gu, L. J., Sun, X. G., Yang, S. H., and Zhang, X. H. (2014) Comprehensive analysis of patched domain-containing genes reveals a unique evolutionary pattern. *Genet. Mol. Res.* **13**, 7318–7331

59. Kuwabara, P. E., and Labouesse, M. (2002) The sterol-sensing domain: multiple families, a unique role? *Trends Genet.* **18**, 193–201

60. Millard, E. E., Gale, S. E., Dudley, N., Zhang, J., Schaffer, J. E., and Ory, D. S. (2005) The sterol-sensing domain of the Niemann-Pick C1 (NPC1) protein regulates trafficking of low density lipoprotein cholesterol. *J. Biol. Chem.* **280**, 28581–28590

61. Davies, J. P., Levy, B., and Ioannou, Y. A. (2000) Evidence for a Niemann–Pick C (NPC) gene family: identification and characterization of NPC1L1. *Genomics* **65**, 137–145

62. Pu, J., Romanelli, R., Zhao, B., Azar, K. M. J., Hastings, K. G., Nimbal, V., Fortmann, S. P., and Palaniappan, L. P. (2015) Dyslipidemia in special ethnic populations. *Cardiol. Clin.* **33**, 325–333

63. Virani, S. S., Alonso, A., Benjamin, E. J., Bittencourt, M. S., Callaway, C. W., Carson, A. P., Chamberlain, A. M., Chang, A. R., Cheng, S., Delling, F. N., Djousse, L., Elkind, M. S. V., Ferguson, J. F., Fornage, M., Khan, S. S., *et al.* (2020) Heart disease and stroke statistics—2020 update: a report from the American Heart Association. *Circulation* **141**, E139–E596

64. Ohgane, K., Karaki, F., Dodo, K., and Hashimoto, Y. (2013) Discovery of oxysterol-derived pharmacological chaperones for NPC1: implication for the existence of second sterol-binding site. *Chem. Biol.* **20**, 391–402

65. Nowaczyk, M. J. M., and Irons, M. B. (2012) Smith-Lemli-Opitz syndrome: phenotype, natural history, and epidemiology. *Am. J. Med. Genet. C Semin. Med. Genet.* **160C**, 250–262

66. Marsh, A., Wicking, C., Wainwright, B., and Chenevix-Trench, G. (2005) DHPLC analysis of patients with Nevoid Basal Cell Carcinoma Syndrome reveals novel PTCH missense mutations in the sterol-sensing domain. *Hum. Mutat.* **26**, 283

67. Wang, L.-J., and Song, B.-L. (2012) Niemann–Pick C1-Like 1 and cholesterol uptake. *Biochim. Biophys. Acta Mol. Cell Biol. Lipids* **1821**, 964–972

68. Altmann, S. W., Davis, H. R., Zhu, L.-J., Yao, X., Hoos, L. M., Tetzloff, G., Iyer, S. P. N., Maguire, M., Golovko, A., Zeng, M., Wang, L., Murgolo, N., and Graziano, M. P. (2004) Niemann-pick C1 like 1 protein is critical for intestinal cholesterol absorption. *Science* **303**, 1201–1204

69. Prabhu, A. V., Luu, W., Sharpe, L. J., and Brown, A. J. (2016) Cholesterol-mediated degradation of 7-dehydrocholesterol reductase switches the balance from cholesterol to vitamin D synthesis. *J. Biol. Chem.* **291**, 8363–8373

70. Prabhu, A. V., Luu, W., Li, D., Sharpe, L. J., and Brown, A. J. (2016) DHCR7: a vital enzyme switch between cholesterol and vitamin D production. *Prog. Lipid Res.* **64**, 138–151

71. Wassif, C. A., Maslen, C., Kachilele-Linjewile, S., Lin, D., Linck, L. M., Connor, W. E., Steiner, R. D., and Porter, F. D. (1998) Mutations in the human sterol D 7 -reductase gene at 11q12-13 cause Smith-Lemli-Opitz syndrome. *Am. J. Hum. Genet.* **63**, 55–62

72. Vanier, M. T. (2015) Complex lipid trafficking in Niemann-Pick disease type C. *J. Inherit. Metab. Dis.* **38**, 187–199

73. Carstea, E. D., Morris, J. A., Coleman, K. G., Loftus, S. K., Zhang, D., Cummings, C., Gu, J., Rosenfeld, M. A., Pavan, W. J., Krizman, D. B., Nagle, J., Polymeropoulos, M. H., Sturley, S. L., Ioannou, Y. A., Higgins, M. E., *et al.* (1997) Niemann-Pick C1 disease gene: homology to mediators of cholesterol homeostasis. *Science* **277**, 228–231

74. Johnson, R. L., Rothman, A. L., Xie, J., Goodrich, L. V., Bare, J. W., Bonifas, J. M., Quinn, A. G., Myers, R. M., Cox, D. R., Epstein, E. H., and Scott, M. P. (1996) Human homolog of patched, a candidate gene for the basal cell nevus syndrome. *Science* **272**, 1668–1671